Environmental Science & Technology

pubs.acs.org/est

Article

Determination of Characteristic vs Anomalous $^{135}Cs/^{137}Cs$ Isotopic Ratios in Radioactively Contaminated Environmental Samples

Dorian Zok, Tobias Blenke, Sandra Reinhard, Sascha Sprott, Felix Kegler, Luisa Syrbe, Rebecca Querfeld, Yoshitaka Takagai, Vladyslav Drozdov, Ihor Chyzhevskyi, Serhii Kirieiev, Brigitte Schmidt, Wolfram Adlassnig, Gabriele Wallner, Sergiy Dubchak, and Georg Steinhauser*

Cite This: *Environ. Sci. Technol.* 2021, 55, 4984−4991

Read Online

ACCESS | Metrics & More | Article Recommendations | Supporting Information

ABSTRACT: A contamination with the ubiquitous radioactive fission product ^{137}Cs cannot be assigned *per se* to its source. We used environmental samples with varying contamination levels from various parts of the world to establish their characteristic $^{135}Cs/^{137}Cs$ isotope ratios and thereby allow their distinction. The samples included biological materials from Chernobyl and Fukushima, historic ashed human lung tissue from the 1960s from Austria, and trinitite from the Trinity Test Site, USA. After chemical separation and gas reaction shifts inside a triple quadrupole ICP mass spectrometer, characteristic $^{135}Cs/^{137}Cs$ isotope signatures (all as per March 11, 2011) were obtained for Fukushima- (∼0.35) and Chernobyl-derived (∼0.50) contaminations, in agreement with the literature for these contamination sources. Both signatures clearly distinguish from the characteristic high ratio (1.9 ± 0.2) for nuclear-weapon-produced radiocesium found in human lung tissue. Trinitite samples exhibited an unexpected, anomalous pattern by displaying a low (<0.4) and nonuniform $^{135}Cs/^{137}Cs$ ratio. This exemplifies a ^{137}Cs-rich fractionation of the plume in a nuclear explosion, where ^{137}Cs is a predominant species in the fireball. The onset of ^{135}Cs was delayed because of the longer half-life of its parent nuclide ^{135}Xe, causing a spatial separation of gaseous ^{135}Xe from condensed ^{137}Cs, which is the reason for the atypical $^{135}Cs/^{137}Cs$ fractionation in the fallout at the test site.

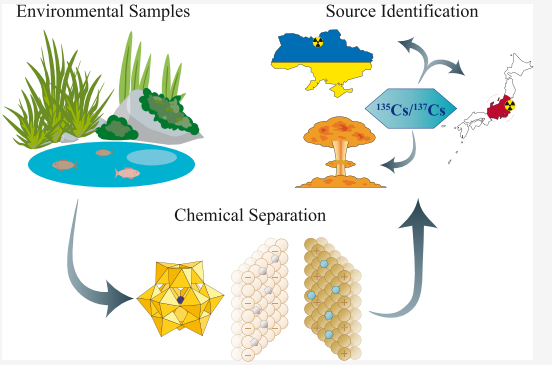

INTRODUCTION

Cesium-137 ($T_{1/2}$ = 30.1 y) is a high-yield product of nuclear fission and one of the most notorious radioactive contaminants globally. It has been released in great amounts in the course of nuclear testing as well as all the major nuclear accidents in Fukushima (2011),[1,2] Chernobyl (1986),[3] Windscale (1957), and Kyshtym (1957),[4] thus making it a ubiquitous environmental contaminant. Due to its many sources, ^{137}Cs alone cannot be assigned to its source(s) but requires the use of sophisticated analytical techniques to include difficult-to-measure, long-lived ^{135}Cs ($T_{1/2} = 2.3 \times 10^6$ y) to establish a characteristic $^{135}Cs/^{137}Cs$ isotopic ratio. This ratio is becoming a powerful tool for the assignment of an environmental radiocesium contamination to its source and thereby may help reveal crucial forensic information such as the legal background or age of said contamination.[5] Even migration pathways or mixing of sources could be resolved by application of $^{135}Cs/^{137}Cs$ ratios as isotopic fingerprints. While the use of ratios of typical actinide isotopes of plutonium or uranium is well established in nuclear forensics, the use of the radiocesium system $^{135}Cs/^{137}Cs$ is fairly novel, rapidly expanding, and not yet fully explored.[6−10] In the first years after a nuclear accident, some forensic insight can be derived from establishing the ratio of shorter-lived ^{134}Cs ($T_{1/2}$ = 2.1 y) to ^{137}Cs. However, the applicability of this ratio is not only limited by the short half-life of ^{134}Cs but also by the nuclear production routes of the radiocesium isotopes. ^{134}Cs is produced by neutron capture of the stable fission product ^{133}Cs, which is the end-point of the 133 isobar. In contrast, ^{137}Cs is a fission product cumulating any parent nuclides on the 137 isobar. Last, ^{135}Cs is a direct fission product, but its onset is greatly suppressed by its parent nuclide ^{135}Xe that has a giant cross section (2.6×10^6 b) for thermal neutron capture.[11] Depending on the neutron flux density inside the reactor, ^{135}Xe will be burnt off to a significant degree and thus prevent the onset of ^{135}Cs. This scenario refers to operating nuclear reactors in particular. However, whenever the reactor is shut down, ^{135}Xe will be produced by its parent ^{135}I ($T_{1/2}$ = 6.6 h) after the neutron flux has stopped, and ^{135}Xe ($T_{1/2}$ = 9.1 h) will be allowed to decay into its daughter ^{135}Cs. The same scenario applies to the explosion of a nuclear warhead, with its very short duration and intense as well as high-energy neutron flux that allows for the

Received: January 8, 2021
Revised: February 12, 2021
Accepted: February 17, 2021
Published: March 12, 2021

formation of ^{135}Cs. In contrast to ^{134}Cs and ^{137}Cs, both of which are produced as a function of burnup, the onset of ^{135}Cs mainly depends on the (lack of) neutron action on its parent. This adds much more distinct features to the ^{135}Cs/^{137}Cs fingerprint as compared to the easy-to-measure ^{134}Cs/^{137}Cs ratio, which is fairly similar for fuel with similar burnup and cooling times.[12]

The distinct nuclear production routes of ^{135}Cs and ^{137}Cs allow for a characteristic ratio of ^{135}Cs/^{137}Cs that acts as a fingerprint for a particular source. It allows for a fine distinction between contaminations caused by nuclear weapon fallout[13,14] and the releases from the Chernobyl nuclear power plant (ChNPP) or Fukushima Daiichi nuclear power plant (FDNPP).[8,15−17] Naturally, global nuclear weapons fallout affected mainly the entire northern hemisphere and hence contributed minute amounts of radiocesium to the Chernobyl and Fukushima signature. Even the fallout of Chernobyl-derived radiocesium was observed in small but discernible amounts in Japan in 1986.[18] In any case, our samples were so highly contaminated that the effects of this mixing of signatures can be deemed negligible. When using highly contaminated materials (and thus large amounts of the analyte), it even allows a distinguishing between the different reactor blocks and spent fuel pools at FDNPP.[6,19] With lower amounts of the analyte, this distinction is much more challenging. For this study, living organisms (moss, fish) were chosen to represent Chernobyl's and Fukushima's contamination because these must have taken up bioavailable radiocesium from the environment.

Despite all advantages, measurement of the ^{135}Cs remains challenging. While activities of ^{134}Cs and ^{137}Cs are easily determinable by gamma spectrometry,[11] ^{135}Cs is a long-lived, pure β^--emitter that exhibits low specific activities in environmental concentrations. Therefore, classical radiometric methods are usually not applicable for this nuclide. Furthermore, also mass spectrometric methods face obstacles in the measurement of radiocesium isotopes because of interfering stable barium isotopes ^{135}Ba (natural abundance 6.59%) and ^{137}Ba (11.23%) and low radiocesium concentrations at moderate contamination levels. Thus, a multistep chemical separation prior to the measurement is imperative, starting with ion exchange reactions of Cs with ammonium molybdophosphate (AMP), followed by anionic and cationic ion exchange resins.[6,7] However, formation of polyatomic interferences in the plasma of an inductively coupled plasma mass spectrometer (ICP-MS) remains a threat for the analysis of trace amounts of Cs isotopes. This is mainly true for Mo (^{95}Mo^{40}Ar$^+$, ^{97}Mo^{40}Ar$^+$) that has been introduced into the sample in the form of AMP. Further possible interferences include oxides of ^{121}Sb and ^{119}Sn, as well as hydrides of $^{134/136}$Xe and $^{134/136}$Ba.[6,14] Therefore, molybdates, along with antimonates and stannates, have to be separated from Cs by anionic exchange resins.

Triple quadrupole ICP-mass spectrometry (ICP-QQQ-MS) has been proven a powerful tool to measure the ^{135}Cs/^{137}Cs ratio by taking advantage of chemical shift reactions.[20] Quadrupoles 1 and 3 are set on the detection at an m/z ratio of 135 and 137, respectively, while the central mass filter constitutes a reaction chamber with a gas filling of He and a low percentage of N_2O.[21] Residual barium is likely to form an oxide and hence may be suppressed by several orders of magnitude. In contrast, Cs passes the filter nearly reactionlessly. A combination of chemical separation and online gas reactions warrants the detection of even small amounts of ^{135}Cs and ^{137}Cs. The objective of this study was to investigate the applicability of the ^{135}Cs/^{137}Cs isotopic fingerprinting technique to common (Chernobyl, Fukushima) and understudied sources of radiocesium (nuclear weapons fallout) and to find out if the various sources can be discerned by a unique fingerprint.

MATERIALS

Sample Materials. Three major sources of environmental radiocesium were to be covered in this study: atmospheric nuclear weapons fallout as well as the major nuclear accidents at ChNPP and FDNPP. For the analysis, we collected hyperaccumulating mosses from the areas around ChNPP and FDNPP. Some species of moss are notorious for their high affinity for Cs.[22] Furthermore, permission was obtained to catch fish in the Chernobyl cooling pond as a representative of animal tissue, which, due to its higher fat content, is more challenging in the chemical treatment than plant materials. Samples with a "pure" nuclear weapons fallout contamination are hardly accessible nowadays. To exemplify ^{135}Cs/^{137}Cs signatures of nuclear weapons fallout, we selected historic materials: historic ashed human lung tissue from the 1960s from Austria as well as commercially available samples of trinitite. Trinitite is a mineral that formed upon the first nuclear weapons test at the Trinity Test Site, NM, USA, and consists of molten glass, crystalline debris, and radionuclides. Before the Trinity Test Site was closed to the public, large amounts of trinitite were collected by mineral and nuclear enthusiasts and are traded still today.

Samples from Chernobyl, Ukraine. Two types of samples were taken from the Chernobyl Exclusion Zone (CEZ), Ukraine. Moss samples were collected in October 2018 in the vicinity of the cooling pond of ChNPP. Wels catfish (*Silurus glanis*) and zander (*Sander lucioperca*) were caught in October 2018, too. Details on samples and sampling locations are compiled in the Supporting Information (SI), see Table S1 and Figures S1 and S2. For the present study, muscle meat from the back of the fish was used.

Samples from Fukushima, Japan. Mosses were collected in Fukushima and neighboring prefectures (Table S2, Figure S3) in July 2019. Samples were weighed, dried at 50 °C, homogenized in a ball mill, and sterilized by autoclave. For a safe transportation to Germany and obeying regulations, they were processed to be sealed products in solidified gel (agar−agar gel). Upon arrival, the gel was removed by heating at 80 °C for 36 h. Afterward, the dried gel film was carefully removed from the moss for measurement. All measurements of radioactivity in sample were conducted in Germany.

Trinitite from the Trinity Test Site, USA. Two specimens of trinitite were purchased form the Mineralogical Research Co. Both samples were recovered from the Trinity Test Site (Tularosa Basin, Alamogordo), NM, USA, where the first nuclear warhead was tested on July 16, 1945. Specifications of the trinitites can be found in Table S3 and Figure S4.

Historic Ashed Human Lung Tissue from Vienna. Sample materials from a historic study of human lung tissue were made available to this study.[23−26] The donators passed away in the early 1960s. The tissue samples were collected by the late Prof. Schönfeld of University of Vienna, ashed, and then analyzed for gamma-emitting fission products. Samples were then put on storage at the University of Vienna from where they were now retrieved (data in Table S4). Five samples from 1963 to 1965 (thus covering the time range of the maximum fallout) were pooled to obtain measurable radiocesium concentrations.

IAEA Reference Materials. For the internal and external comparability of our measurements, homogeneous and commercially available reference materials provided by IAEA

https://dx.doi.org/10.1021/acs.est.1c00180
Environ. Sci. Technol. 2021, 55, 4984−4991

were used. Both reference materials, IAEA-372 (radionuclides in grass) and IAEA-330 (radionuclides in spinach), are from the same farm in Polesskoe, Kiev, Ukraine, and are often used as reference materials for this type of study as they exhibit a $^{135}Cs/^{137}Cs$ ratio characteristic for Chernobyl radiocesium fallout (Table S5).

METHODS

Sample Preparation. Organic samples were incinerated in porcelain crucibles for the utmost removal of the organic matrix. First, they were heated up in a muffle furnace to 350 °C (2 h) and held at this temperature for 2 h. Then, the furnace was heated to 450 °C (2 h) and held for 12 h for final ashing. After cooling, the ashed material was transferred into 110 mL PTFE vessels of the microwave digestion system MARS 6 from CEM Corporation using 4 × 2.5 mL of supra-pure HNO_3 (69%, ROTIPURAN, Supra, Carl Roth). Digestion was performed using a temperature ramp from room temperature to 160 °C within 20 min. This temperature was held for 30 min. After cooling, the solutions were filtered through a Whatman Filter 602 H1/2 (pore size <2 μm) and transferred into PFA vessels. The digestion vessels were washed out with 4 × 5 mL of Merck Millipore Milli-Q water (18.2 MΩcm). Digestion and wash solutions were combined and evaporated to dryness. The residue was redissolved with 10 mL of 1.6 M HNO_3. A 50 μL aliquot was taken as a recovery yield tracer. The tracer was diluted to 2 mL of a 2% HNO_3 solution with sub-boiled HNO_3 for concentration determination. Sub-boiled HNO_3 was prepared from 65% HNO_3 (ROTIPURAN, p.a., Carl Roth).

Trinitite samples were crushed to small particles and put into a 120 mL Savillex PFA vessel. Three × 20 mL HF (48%, Merck EMSURE, ACS) was added and evaporated to dryness after each step. Filtration, evaporation, and recovery yield determination were performed as above.

Cs Separation by AMP. For the Cs extraction from the dissolved sample matrices, solid ammonium molybdophosphate powder ($H_{12}Mo_{12}N_3O_{40}P{\cdot}xH_2O$ (x ≈ 3); AMP; ACS > 95%) from Alfa Aesar was used. Solutions were brought to 50 mL of 1.6 M HNO_3, and 35 mg of AMP was added. The solution was stirred for 1 h. Thereafter, the samples were filtered thought a 1.2 μm cellulose acetate syringe filter. The AMP(Cs) was dissolved by adding 10 mL of 1.5 M NH_3 solution (20%, ROTIPURAN Supra, Carl Roth) and collected in a PFA breaker.[6,21]

Anion Exchange Resin. In order to remove the interfering elements Mo, Sb, and Sn, the anion exchange resin Dowex 1-X8 (100−200 mesh) from Alfa Aesar was used. Prior to use, the 2 mL resin was cleaned for each sample with 4 × 5 mL of 1.5 M NH_3. Then, the anion exchange resin was conditioned with 2 × 5 mL of 1.5 M NH_3, followed by loading the dissolved AMP(Cs) solution. As a cation, Cs^+ is not trapped in this resin. Residual Cs^+ ions were eluted from the resin by adding 2 × 5 mL of 1.5 M NH_3. Loading and elution solutions were combined and evaporated to dryness in a PFA beaker. Redissolution was achieved with 10 mL of 0.15 M NH_3 as suggested by Zheng et al.[6,21]

Cation Exchange Resin. The cation exchange resin AG 50W-X8 (100−200 mesh) from BioRad Laboratories, Inc. was precleaned by using 4 M sub-boiled HNO_3 to remove unwanted cations during resin production (2 × 5 mL).[27] A volume of 2 mL of the cleaned AG 50W-X8 was packed into an empty column and used for one sample.

The resin was conditioned with 2 × 5 mL 0.15 M NH_3, followed by loading of the redissolved sample solution obtained from the previously described anion exchange procedure. The resin was washed with 2 × 5 mL 0.15 M NH_3 and 18.2 MΩcm H_2O, respectively. Elution of Cs^+ was performed with 6 × 5 mL of 1.5 M sub-boiled HCl (prepared from 37% HCl, ROTIPURAN, p.a., Carl Roth). The Cs containing eluate was collected in a PFA beaker and evaporated to dryness. The dried residue was redissolved in 2 mL of 2% HNO_3. An aliquot of 50 μL was taken for the final calculation of the recovery rate.[6,21]

Gamma Spectrometry for ^{137}Cs Determination. All samples were measured on high-purity germanium (HPGe) detectors at the Institute of Radioecology and Radiation Protection in Hannover, Germany (volume 131 cm^3, relative efficiency 28%, FWHM at 1332 kev of 1.9 keV). Spectra were evaluated using Genie 2000 software from Mirion Technologies, Inc. The certified multinuclide gamma-ray emitting solution QCY-48 from Eckhart and Ziegler Nuclitec GmbH, Germany, was used to calibrate the detector efficiency.

Mass Spectrometry Using ICP-QQQ-MS. Concentrations and isotope ratios were measured using an Agilent 8900 Triple Quadrupole ICP-MS coupled to an SPS4 autosampler using MassHunter 4.4 software, all from Agilent Technologies, Inc. All measurement solutions were prepared from Milli-Q H_2O (18.2 MΩcm) and sub-boiled HNO_3.

Element concentrations as well a recovery rates were measured in a single quadrupole mode without reaction gas. Isotope ratios were measured in triple quadrupole mode with a mixture of He (5N, Linde GmbH) and N_2O (2N, CANGas, Messer Group GmbH) as reactions gas. Parameters are listed in the Supporting Information, Tables S6−S8. Measured values were corrected with a very low processing blank and acid blank (both lower than 1 cps), decay correction of ^{137}Cs to the Fukushima nuclear accident (March 11, 2011), and using the exponential law for mass bias correction.

Residual Ba content after full separation was checked by ICP-MS and was found low enough not to interfere significantly. Mass bias of the plasma was corrected with an external 5 ppb europium reference solution (1000 mg/L, Alfa Aesar) spiked to a blank processed eluate to achieve a comparable matrix like the samples (eq 1 and 2). The β value for this system and measurement was −1.0896,; the reference was the natural Eu ratio.[28]

$$\left(\frac{^{135}Cs}{^{137}Cs}\right)_{corrected} = \left(\frac{^{135}Cs}{^{137}Cs}\right)_{measured} \times \left[\frac{M(^{135}Cs)}{M(^{137}Cs)}\right]^{\beta} \quad (1)$$

$$\beta = \left(\frac{\ln[(^{151}Eu/^{153}Eu)_{reference}/(^{151}Eu/^{153}Eu)_{measured}]}{\ln[(M^{151}Eu)/(M^{153}Eu)]}\right) \quad (2)$$

RESULTS AND DISCUSSION

^{137}Cs Activities and Content of the Samples. The samples analyzed in this study covered not only a wide range of sources but also activity concentrations. Therefore, suitable amounts were chosen to achieve at least some tens of becquerel for a sufficient counting statistic during ICP-QQQ-MS measurement. Activity concentrations of ^{137}Cs obtained by gamma spectrometry (unless certified) are tabulated in Tables S1−S5. Moss samples from Fukushima exhibited the highest activity concentration with more than 2500 Bq/g fresh weight. Similarly, the fish and moss samples collected from CEZ showed reasonably high ^{137}Cs activity concentrations. Very low activities

https://dx.doi.org/10.1021/acs.est.1c00180
Environ. Sci. Technol. 2021, 55, 4984−4991

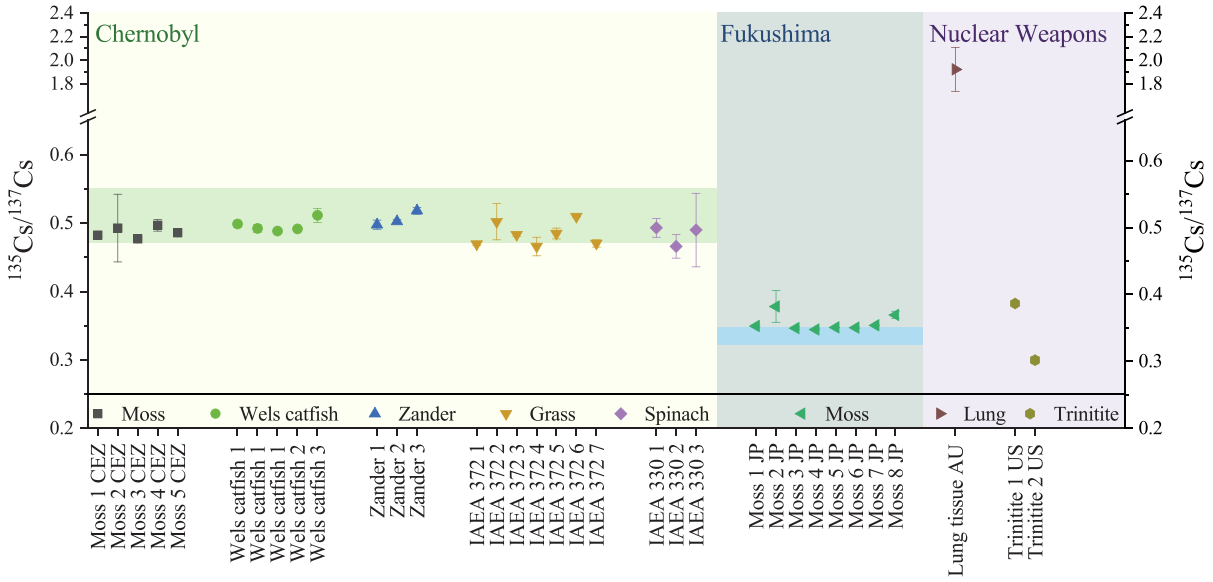

Figure 1. $^{135}Cs/^{137}Cs$ isotopic ratios for samples from different locations. Samples are classified for their origin in Chernobyl, Fukushima, or nuclear weapons. All values are date corrected to March 11, 2011 for better comparison. Darker areas showing previously published values for the $^{135}Cs/^{137}Cs$ ratio for Chernobyl and Fukushima by other techniques and groups.

are found in the samples of ashed human lung tissue with only millibecquerels per gram. The choice of the amount of sample material needed for ICP-QQQ-MS measurements depended on the ^{137}Cs activities or availability of said material.

Concentrations of Analytes and Recovery Yields. Aliquots were taken before and after the separation to determine concentrations and yields of the key elements Cs and its main isobaric interference Ba, as well as Mo, Sn, and Sb. Exact values are listed in Tables S9 and S10 in the SI. Generally, the purification process removed approximately 90% of the initial amount of interfering Mo, Sn, and Sb. For the most sample types, their initial content is just in the range of some tens of nanograms. A few samples appeared to be slightly contaminated by Mo due to the use of AMP. Nevertheless, the residual concentrations proved low enough to not interfere with the determination of the $^{135}Cs/^{137}Cs$ ratio. Barium removal in the separation proved to be highly efficient (99.7%). Losses of Cs through the entire purification process were in the range of 20%. In any case, please note that the initial Cs content is relatively low with only some hundreds of nanograms, compared to the initial Ba content (up to several milligrams). This explains why instrumental suppression of Ba inside the ICP-QQQ-MS alone is insufficient, making the chemical separation crucial to decreasing the Ba content into the lower nanogram range prior to measurement.

$^{135}Cs/^{137}Cs$ Isotopic Ratios. Calculated values for the $^{135}Cs/^{137}Cs$ ratio are shown in Figure 1, together with reference values from the literature (darker area).[6,7,15,16,21] Tabulated values can be found in Table 2, together with activities and the masses of both nuclides. Since the $^{135}Cs/^{137}Cs$ ratio depends on the fairly short half-life of ^{137}Cs, the ratio shifts significantly over the decades. For certain samples, e.g., Chernobyl, Fukushima, or trinitite, an exact release date can be defined. However, for the lung tissue, this is trickier, because the lungs have likely accumulated radiocesium over several years. Table S11 and Figure S5 illustrate the shift of the ratio over time in tabulated and graphical form. Chernobyl samples were compared with the isotope ratio of reference material IAEA-375. This reference material has become the most used international reference for

Table 1. IAEA Reference Materials Comparison with Already Published Values[a]

reference	$^{135}Cs/^{137}Cs$	*n*	publication	method
IAEA-330	0.52 ± 0.005	2	Snow[13]	TIMS
	0.55 ± 0.031	4	Zheng[29]	ICP-QQQ-MS
	0.56 ± 0.02	3	Dunne[30]	TIMS
	0.58 ± 0.001	3	Bu[20]	TIMS
	0.56 ± 0.02	1	Zhu[31]	ICP-QQQ-MS
	0.48 ± 0.024	3	our work	ICP-QQQ-MS
IAEA-372	0.574 ± 0.008	7	Bu[20]	TIMS
	0.483 ± 0.031	7	our work	ICP-QQQ-MS

[a]Ratios were decay corrected to March 11, 2011. Errors are given with 2 s.d.

$^{135}Cs/^{137}Cs$ isotope measurements. Several groups already published values for this material with values ranging from 0.48 to 0.55 (corrected to March 11, 2011).[6,7,15,16,21] Unfortunately, IAEA-375 is no longer commercially available. As alternatives, IAEA-330 and IAEA-372 that were both contaminated by the Chernobyl nuclear accident are still available and have similar average values ranging between 0.523 and 0.525 (as of March 11, 2011; see Table 1).[14] In the discussion of $^{135}Cs/^{137}Cs$ fingerprints of releases from various sources, the time shift of the ratio complicates comparison of the data. While one may argue that Chernobyl samples should ideally be decay-corrected to April 26, 1986, and Fukushima samples should be decay-corrected to March 11, 2011, we chose the most recent nuclear accident (i.e., the Fukushima) as the uniform reference date for all ratios in this paper. This shows that, whatever the source, their fingerprint remains distinguishable today. On the downside of this uniform reference date, the values spread over a wider range and their uncertainties increase.

Generally, all of our CEZ samples are within the (lower) range of previously published Chernobyl $^{135}Cs/^{137}Cs$ isotope ratios with a value around 0.490 (Figure 1). Deviations are likely due to traces of residual Ba on the resin. Both IAEA reference materials are represented with 10 samples with a slight spread around 0.483. Mosses and fish that were collected inside the

https://dx.doi.org/10.1021/acs.est.1c00180
Environ. Sci. Technol. 2021, 55, 4984−4991

Table 2. $^{135}Cs/^{137}Cs$ Isotope Ratio Values of All Samples Including Analytical Uncertainties[a]

sample	$^{135}Cs/^{137}Cs$	uncert. (±)	^{135}Cs activity [Bq]	^{135}Cs mass [pg]	^{137}Cs activity [Bq]	^{137}Cs mass [pg]
wels catfish 1	0.499	0.004	1.2×10^{-4}	2.9	18.88	5.9
wels catfish 1	0.492	0.006	1.3×10^{-4}	2.9	19.26	6.0
wels catfish 1	0.488	0.003	1.2×10^{-4}	2.9	19.06	5.9
wels catfish 2	0.491	0.002	7.4×10^{-5}	1.7	11.49	3.6
wels catfish 3	0.511	0.010	6.1×10^{-5}	1.4	9.07	2.8
moss 1 CEZ	0.482	0.003	4.2×10^{-5}	1.0	6.57	2.0
moss 2 CEZ	0.493	0.050	8.0×10^{-5}	1.9	12.32	3.8
moss 3 CEZ	0.477	0.001	8.5×10^{-5}	2.0	13.50	4.2
moss 4 CEZ	0.497	0.009	3.1×10^{-4}	7.1	46.91	14.6
moss 5 CEZ	0.486	0.001	1.0×10^{-4}	2.4	16.14	5.0
zander 1	0.498	0.007	1.9×10^{-4}	4.3	28.47	8.9
zander 2	0.502	0.003	5.9×10^{-5}	1.4	8.96	2.8
zander 3	0.518	0.005	5.3×10^{-5}	1.2	7.76	2.4
IAEA 372 1	0.469	0.002	8.6×10^{-5}	2.0	13.91	4.3
IAEA 372 2	0.502	0.026	1.0×10^{-4}	2.3	15.14	4.7
IAEA 372 3	0.483	0.002	9.1×10^{-5}	2.1	14.24	4.4
IAEA 372 4	0.466	0.014	8.8×10^{-5}	2.0	14.26	4.4
IAEA 372 5	0.485	0.008	9.1×10^{-5}	2.1	14.26	4.4
IAEA 372 6	0.509	0.001	1.9×10^{-4}	4.5	28.68	8.9
IAEA 372 7	0.470	0.005	8.8×10^{-5}	2.0	14.12	4.4
IAEA 330 1	0.493	0.014	4.0×10^{-5}	0.9	6.20	1.9
IAEA 330 2	0.466	0.017	3.8×10^{-5}	0.9	6.20	1.9
IAEA 330 3	0.490	0.054	4.7×10^{-5}	1.1	7.27	2.3
moss 1 JP	0.349	0.001	1.3×10^{-2}	302	2830	880
moss 2 JP	0.378	0.023	6.1×10^{-3}	142	1231	383
moss 3 JP	0.346	0.002	7.9×10^{-3}	182	1721	535
moss 4 JP	0.344	0.001	6.7×10^{-3}	156	1476	459
moss 5 JP	0.347	0.001	6.2×10^{-3}	145	1361	423
moss 6 JP	0.347	0.001	1.1×10^{-2}	248	2334	725
moss 7 JP	0.351	0.001	1.1×10^{-3}	26.2	244	75.9
moss 8 JP	0.366	0.005	3.8×10^{-4}	8.9	79.72	24.8
lung AT	1.922	0.187	9.1×10^{-5}	2.1	3.60	1.1
trinitite 1 US	0.382	0.003	1.7×10^{-4}	3.9	32.94	10.2
trinitite 2 US	0.300	0.006	2.3×10^{-4}	5.3	58.10	18.1

[a]Values are date-corrected to March 11, 2011.

CEZ are in good agreement with both reference materials. After more than 30 years since the accident, the environment of the CEZ and its organisms still exhibit the identifiable signature of this release. This makes the $^{135}Cs/^{137}Cs$ ratio a suitable forensic tool for the assignment of a contamination to this accident.

Due to operational and design differences, nuclear power plants are distinguishable via the $^{135}Cs/^{137}Cs$ ratio. Fukushima moss samples exhibit a ratio around 0.358. No IAEA reference material from this region is yet available. Nevertheless, the already published measured values for this ratio are in the range around 0.34−0.36 and hence in good agreement with our data.[21] It should be noted that, unlike Chernobyl, Fukushima's releases are not uniform but involve three different sources, i.e., three reactors. With highly contaminated samples, the minor but characteristic fluctuations of the $^{135}Cs/^{137}Cs$ can be resolved and used to assign the contamination to one reactor.[21] Higher Fukushima-derived ratios were also measured in marine sediments in the Pacific Ocean with values ranging from 0.36 to 0.45.[14] In any case, contaminations caused by the two most notable civilian accidents at Chernobyl and Fukushima are very well distinguishable via the $^{135}Cs/^{137}Cs$ ratio because the gap range between both signatures is big enough.

Fallout from atmospheric nuclear explosions in the 20th century constitutes a third and ubiquitous source of radiocesium. The $^{135}Cs/^{137}Cs$ ratio found in historic ashed human lung tissue samples from the early 1960s was higher (1.9) and thus clearly distinct from Chernobyl's or Fukushima's fingerprints. This value is in agreement with what has been reported previously.[7,8] The higher ratio comes expected as "neutron burning" of ^{135}Xe (the parent nuclide of ^{135}Cs) does not occur in a nuclear explosion due to the short duration of the nuclear chain reaction. It can be expected that the contamination of this historic lung tissue was dominated by nuclear explosions fallout (whereas the 1957 accidents at Windscale and Kyshtym were likely local rather than global sources of atmospheric contamination).

Materials contaminated by nuclear weapons fallout, including both rock samples from the Trinity Test Site, were expected to resemble the high $^{135}Cs/^{137}Cs$ ratio that is characteristic of nuclear weapons fallout of ^{239}Pu warheads. The fast neutron cumulative fission yields of ^{239}Pu are 7.54% for the 135-isobar and 6.35% for the 137-isobar, causing a theoretical $^{135}Cs/^{137}Cs$ ratio of 1.19 for this type of sample material at the time of the detonation.[29] However, in our measurements, both samples exhibited a significantly lower ratio (decay-corrected to 2011 $^{135}Cs/^{137}Cs$ 0.382 ± 0.003 and 0.300 ± 0.006, respectively, or <0.1 at the time of the explosion). The hypothesis of a high $^{135}Cs/^{137}Cs$ ratio hence could *not* be confirmed for the two

https://dx.doi.org/10.1021/acs.est.1c00180
Environ. Sci. Technol. 2021, 55, 4984−4991

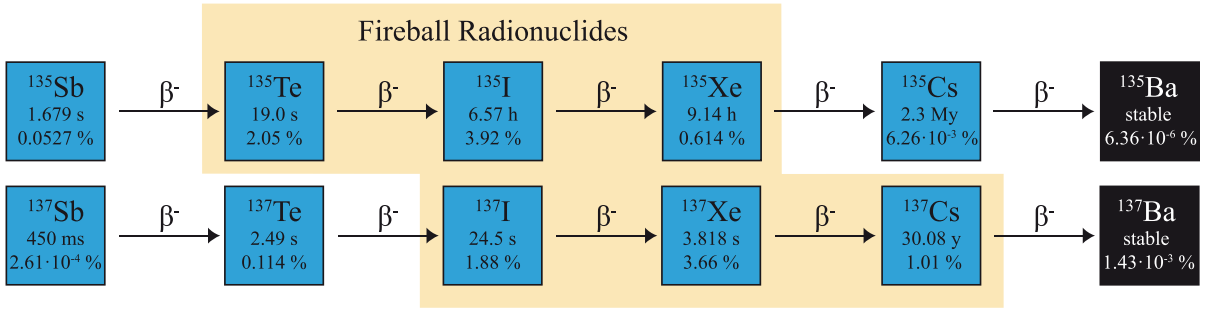

Figure 2. Isobaric decay chains leading to ^{135}Cs and ^{137}Cs, respectively, show that ^{137}Cs is directly produced inside the fireball of a nuclear blast, whereas ^{135}Cs is not. Data presented for each nuclide include half-life and independent fast neutron fission yield of ^{239}Pu in %. Data taken from ref 34.

trinitite samples. The only explanation for this anomalous behavior is a fractionation of radiocesium isotopes that relates to the gaseous nature of some precursor isotopes in the fireball. Not all fission products are formed (either directly by fission or subsequently by the decay of short-lived precursors) during the existence of the fireball following the nuclear explosion. Dominant nuclides in the fireball were those with a sufficient neutron excess, including ^{137}Cs.[30] However, ^{135}Cs with its low neutron excess was not a significant radionuclide constituent of the fireball, but rather its relatively long-lived parent nuclides ^{135}Xe ($T_{1/2}$ = 9.14 h), ^{135}I ($T_{1/2}$ = 6.57 h), or ^{135}Te ($T_{1/2}$ = 19 s; Figure 2). The noble gas ^{135}Xe disperses quickly before it decays to ^{135}Cs, whereas ^{137}Cs condenses together with inert molten material that finally constitutes the glassy matrix of trinitite. The volatility of precursor nuclides has been identified as the reason for unexpected nuclide fractionations previously.[30] Stable isotopic anomalies have also been observed on various occasions where a nuclear release impacted the natural isotopic occurrences.[31,32] For cesium isotopes, only the complementary pattern of this isotopic fractionation had been observed previously:[33] in environmental samples taken from more remote locations downwind from the test site, the ^{135}Cs-rich "far-end" with samples exhibiting a high ^{135}Cs/^{137}Cs ratio.[33] Here, to the best of our knowledge, we observe for the first time the complementary ^{137}Cs-rich "near-end" showing the opposite pattern with a low ^{135}Cs/^{137}Cs signature. It shows that isotopic fractionation can occur in environmental samples taken in close proximity to the source (e.g., trinitite), leading to deviations that are not observed in samples from more remote locations (e.g., human lung tissue). The impact of this fractionation on the ^{135}Cs/^{137}Cs fingerprint is severe. Instead of exhibiting a high ^{135}Cs/^{137}Cs ratio typical for nuclear weapons fallout (range 2.0−2.7 in the literature, 1.9 in our study), the trinitite samples studied here exhibit a low ratio that is regarded characteristic for reactors. The nonuniformity of the ^{135}Cs/^{137}Cs fingerprint of both samples in this study reflects the great variability of the extent to which ^{135}Cs has been incorporated into the trinitite (vs ^{135}Xe that was blown away with the wind before it decayed to ^{135}Cs). This suggests a dependency of the ^{135}Cs/^{137}Cs isotopic ratio on the distance from ground zero of a nuclear blast. We propose a method to estimate the distance/location of a radiocesium-contaminated material of a nuclear explosion from ground zero, by analyzing its ^{135}Cs/^{137}Cs fingerprint.

In summary, our results prove the applicability for source attribution of a radiocesium contamination caused by reactor accidents by using the ^{135}Cs/^{137}Cs ratio as an isotopic fingerprint. For nuclear weapons fallout, however, the expected "high" ^{135}Cs/^{137}Cs ratio could only be found in the "remote" sample of historic human lung tissue from Austria. In a highly contaminated trinitite, a fractionation of cesium nuclides could be observed for the first time. This fractionation causes selective enrichment of the "fireball nuclide" ^{137}Cs in the molten glass in the "near end," whereas the ^{135}Cs-rich "far-end" can be observed only at a distance (allowing for the decay of the relatively long-lived mother ^{135}Xe).[33]

Remaining challenges of the applicability of this ^{135}Cs/^{137}Cs fingerprinting include the lack of certified and internationally accepted reference materials for ^{135}Cs/^{137}Cs ratios and the lack of a convention for decay-correction (i.e., a uniform reference date).

■ ASSOCIATED CONTENT

Supporting Information

The Supporting Information is available free of charge at https://pubs.acs.org/doi/10.1021/acs.est.1c00180.

Sample material information for samples from Chernobyl (Table S1), from Fukushima (Table S2), trinitite (Table S3), historic ashed human lung tissue (Table S4), and IAEA Reference Materials (Table S5); measurement parameters for ICP-QQQ-MS measurements (Tables S6−S8); concentrations of elements before and after separation (Mo, Sn, Sb, Table S9; Cs, Ba, Table S10); time shifts (Table S11); pictures of sample materials from CEZ (Figures S1 and S2), Fukushima (Figure S3), trinitite (Figure S4); graphical illustration of the time shifts of ^{135}Cs/^{137}Cs over various decades (Figure S5) (PDF)

■ AUTHOR INFORMATION

Corresponding Author

Georg Steinhauser − *Leibniz Universität Hannover, Institute of Radioecology and Radiation Protection, 30419 Hannover, Germany*; orcid.org/0000-0002-6114-5890; Email: steinhauser@irs.uni-hannover.de

Authors

Dorian Zok − *Leibniz Universität Hannover, Institute of Radioecology and Radiation Protection, 30419 Hannover, Germany*

Tobias Blenke − *Leibniz Universität Hannover, Institute of Radioecology and Radiation Protection, 30419 Hannover, Germany*

Sandra Reinhard − *Leibniz Universität Hannover, Institute of Radioecology and Radiation Protection, 30419 Hannover, Germany*

https://dx.doi.org/10.1021/acs.est.1c00180
Environ. Sci. Technol. 2021, 55, 4984−4991

Sascha Sprott − *Leibniz Universität Hannover, Institute of Radioecology and Radiation Protection, 30419 Hannover, Germany*
Felix Kegler − *Leibniz Universität Hannover, Institute of Radioecology and Radiation Protection, 30419 Hannover, Germany*
Luisa Syrbe − *Leibniz Universität Hannover, Institute of Radioecology and Radiation Protection, 30419 Hannover, Germany*
Rebecca Querfeld − *Leibniz Universität Hannover, Institute of Radioecology and Radiation Protection, 30419 Hannover, Germany*
Yoshitaka Takagai − *Fukushima University, Faculty of Symbiotic Systems Science, Fukushima 960-1296, Japan;* orcid.org/0000-0002-7760-5636
Vladyslav Drozdov − *State Specialized Enterprise "Ecocentre" (SSE "Ecocentre"), Chernobyl 07270, Ukraine*
Ihor Chyzhevskyi − *State Specialized Enterprise "Ecocentre" (SSE "Ecocentre"), Chernobyl 07270, Ukraine*
Serhii Kirieiev − *State Specialized Enterprise "Ecocentre" (SSE "Ecocentre"), Chernobyl 07270, Ukraine*
Brigitte Schmidt − *University of Vienna, Faculty of Life Sciences, Cell Imaging and Ultrastructure Research, 1090 Vienna, Austria*
Wolfram Adlassnig − *University of Vienna, Faculty of Life Sciences, Cell Imaging and Ultrastructure Research, 1090 Vienna, Austria*
Gabriele Wallner − *University of Vienna, Faculty of Chemistry, Institute of Inorganic Chemistry, 1090 Vienna, Austria*
Sergiy Dubchak − *State Specialized Enterprise "Radon Association", Kyiv 03083, Ukraine*

Complete contact information is available at: https://pubs.acs.org/10.1021/acs.est.1c00180

Notes

The authors declare no competing financial interest.

■ ACKNOWLEDGMENTS

We thank *Deutsche Forschungsgemeinschaft* (DFG) for funding the project (419819104) of radiocesium analytics and the *Stiftung Prof. Joachim Lenz* for financial support of the Chernobyl sampling campaign. We also thank DFG and the State of Lower Saxony for the acquisition of the ICP-QQQ-MS and JSPS for the scholarship for R.Q. (SP19315).

■ REFERENCES

(1) Povinec, P. P.; Aoyama, M.; Biddulph, D.; Breier, R.; Buesseler, K.; Chang, C. C.; Golser, R.; Hou, X. L.; Ješkovský, M.; Jull, A. J. T.; Kaizer, J.; Nakano, M.; Nies, H.; Palcsu, L.; Papp, L.; Pham, M. K.; Steier, P.; Zhang, L. Y. Cesium, Iodine and Tritium in NW Pacific Waters - a Comparison of the Fukushima Impact with Global Fallout. *Biogeosciences* **2013**, *10* (8), 5481−5496.
(2) United Nations Scientific Committee on the Effects of Atomic. Sources and Effects of Ionizing Radiation; *Report to the General Assembly*; United Nations: New York, 2008.
(3) Steinhauser, G.; Brandl, A.; Johnson, T. E. Comparison of the Chernobyl and Fukushima Nuclear Accidents: A Review of the Environmental Impacts. *Sci. Total Environ.* **2014**, *470*−*471*, 800−817.
(4) Jones, S. Windscale and Kyshtym: A Double Anniversary. *J. Environ. Radioact.* **2008**, *99* (1), 1−6.
(5) Steinhauser, G. Environmental Nuclear Forensics: The Need for a New Scientific Discipline. *Environ. Sci. Pollut. Res.* **2019**, *26* (17), 16901−16903.
(6) Zheng, J.; Tagami, K.; Bu, W.; Uchida, S.; Watanabe, Y.; Kubota, Y.; Fuma, S.; Ihara, S. $^{135}Cs/^{137}Cs$ Isotopic Ratio as a New Tracer of Radiocesium Released from the Fukushima Nuclear Accident. *Environ. Sci. Technol.* **2014**, *48* (10), 5433−5438.
(7) Snow, M. S.; Snyder, D. C. $^{135}Cs/^{137}Cs$ Isotopic Composition of Environmental Samples across Europe: Environmental Transport and Source Term Emission Applications. *J. Environ. Radioact.* **2016**, *151*, 258−263.
(8) Russell, B. C.; Croudace, I. W.; Warwick, P. E. Determination of ^{135}Cs and ^{137}Cs in Environmental Samples: A Review. *Anal. Chim. Acta* **2015**, *890*, 7−20.
(9) Lee, T.; Teh-Lung, K.; Hsiao-Ling, L.; Ju-Chin, C. First Detection of Fallout Cs-135 and Potential Applications of Ratios. *Geochim. Cosmochim. Acta* **1993**, *57* (14), 3493−3497.
(10) Ohno, T.; Muramatsu, Y. Determination of Radioactive Cesium Isotope Ratios by Triple Quadrupole ICP-MS and Its Application to Rainwater Following the Fukushima Daiichi Nuclear Power Plant Accident. *J. Anal. At. Spectrom.* **2014**, *29* (2), 347.
(11) Nagy, P.; Vajda, N.; Pintér, T.; Fél, K. Activities of ^{134}Cs, ^{135}Cs and ^{137}Cs in the Primary Coolant of VVER-440 Reactors. *J. Radioanal. Nucl. Chem.* **2016**, *307* (2), 1045−1053.
(12) Merz, S.; Steinhauser, G.; Hamada, N. Anthropogenic Radionuclides in Japanese Food: Environmental and Legal Implications. *Environ. Sci. Technol.* **2013**, *47* (3), 1248−1256.
(13) Snow, M. S.; Snyder, D. C.; Clark, S. B.; Kelley, M.; Delmore, J. E. ^{137}Cs Activities and $^{135}Cs/^{137}Cs$ Isotopic Ratios from Soils at Idaho National Laboratory: A Case Study for Contaminant Source Attribution in the Vicinity of Nuclear Facilities. *Environ. Sci. Technol.* **2015**, *49* (5), 2741−2748.
(14) Bu, W.; Tang, L.; Liu, X.; Wang, Z.; Fukuda, M.; Zheng, J.; Aono, T.; Hu, S.; Wang, X. Ultra-Trace Determination of the $^{135}Cs/^{137}Cs$ Isotopic Ratio by Thermal Ionization Mass Spectrometry with Application to Fukushima Marine Sediment Samples. *J. Anal. At. Spectrom.* **2019**, *34* (2), 301−309.
(15) Yang, G.; Tazoe, H.; Yamada, M. Rapid Determination of 135Cs and Precise $^{135}Cs/^{137}Cs$ Atomic Ratio in Environmental Samples by Single-Column Chromatography Coupled to Triple-Quadrupole Inductively Coupled Plasma-Mass Spectrometry. *Anal. Chim. Acta* **2016**, *908*, 177−184.
(16) Taylor, V. F.; Evans, R. D.; Cornett, R. J. Preliminary Evaluation of $^{135}Cs/^{137}Cs$ as a Forensic Tool for Identifying Source of Radioactive Contamination. *J. Environ. Radioact.* **2008**, *99* (1), 109−118.
(17) Snow, M. S.; Snyder, D. C.; Delmore, J. E. Fukushima Daiichi Reactor Source Term Attribution Using Cesium Isotope Ratios from Contaminated Environmental Samples. *Rapid Commun. Mass Spectrom.* **2016**, *30* (4), 523−532.
(18) Merz, S.; Shozugawa, K.; Steinhauser, G. Effective and ecological half-lives of ^{90}Sr and ^{137}Cs observed in wheat and rice in Japan. *J. Radioanal. Nucl. Chem.* **2016**, *307*, 1807−1810.
(19) Yang, G.; Tazoe, H.; Yamada, M. ^{135}Cs Activity and $^{135}Cs/^{137}Cs$ Atom Ratio in Environmental Samples before and after the Fukushima Daiichi Nuclear Power Plant Accident. *Sci. Rep.* **2016**, *6* (1), 24119.
(20) Bu, W.; Ni, Y.; Steinhauser, G.; Zheng, W.; Zheng, J.; Furuta, N. The Role of Mass Spectrometry in Radioactive Contamination Assessment after the Fukushima Nuclear Accident. *J. Anal. At. Spectrom.* **2018**, *33* (4), 519−546.
(21) Zheng, J.; Bu, W.; Tagami, K.; Shikamori, Y.; Nakano, K.; Uchida, S.; Ishii, N. Determination of ^{135}Cs and $^{135}Cs/^{137}Cs$ Atomic Ratio in Environmental Samples by Combining Ammonium Molybdophosphate (AMP)-Selective Cs Adsorption and Ion-Exchange Chromatographic Separation to Triple-Quadrupole Inductively Coupled Plasma-Mass Spectrom. *Anal. Chem.* **2014**, *86* (14), 7103−7110.
(22) Zhong, Q.; Du, J.; Puigcorbé, V.; Wang, J.; Wang, Q.; Deng, B.; Zhang, F. Accumulation of Natural and Anthropogenic Radionuclides in Body Profiles of Bryidae, a Subgroup of Mosses. *Environ. Sci. Pollut. Res.* **2019**, *26* (27), 27872−27887.
(23) Schönfeld, T.; Liebscher, K.; Karl, F.; Friedmann, C. Radioactive Fission Products in Lungs. *Nature* **1960**, *185* (4707), 192−193.

(24) Liebscher, K.; Schönfeld, T.; Schaller, A. Concentration of Inhaled Cerium-144 in Pulmonary Lymph Nodes of Human Beings. *Nature* **1961**, *192* (4809), 1308−1308.
(25) Irlweck, K.; Friedmann, C.; Schönfeld, T. Plutonium in the Lungs of Austrian Residents. *Health Phys.* **1980**, *39*, 95−99.
(26) Schönfeld, T.; Friedmann, C. Deposition of Inhaled Fission Products in Lungs and Pulmonary Lymph Nodes of Human Beings - Final Report on Research Project under Contract with the IAEA. *Rep. IAEA-R-156*; International Atomic Energy Agency, 1965.
(27) Russell, B. C.; Croudace, I. W.; Warwick, P. E.; Milton, J. A. Determination of Precise $^{135}Cs/^{137}Cs$ Ratio in Environmental Samples Using Sector Field Inductively Coupled Plasma Mass Spectrometry. *Anal. Chem.* **2014**, *86* (17), 8719−8726.
(28) Isnard, H.; Granet, M.; Caussignac, C.; Ducarme, E.; Nonell, A.; Tran, B.; Chartier, F. Comparison of Thermal Ionization Mass Spectrometry and Multiple Collector Inductively Coupled Plasma Mass Spectrometry for Cesium Isotope Ratio Measurements. *Spectrochim. Acta, Part B* **2009**, *64* (11−12), 1280−1286.
(29) IAEA - Nuclear Data Section. Live Chart of Nuclides. https://www-nds.iaea.org/relnsd/vcharthtml/VChartHTML.html (accessed Nov 18, 2020).
(30) Hanson, S. K.; Pollington, A. D.; Waidmann, C. R.; Kinman, W. S.; Wende, A. M.; Miller, J. L.; Berger, J. A.; Oldham, W. J.; Selby, H. D. Measurements of Extinct Fission Products in Nuclear Bomb Debris: Determination of the Yield of the Trinity Nuclear Test 70 y Later. *Proc. Natl. Acad. Sci. U. S. A.* **2016**, *113* (29), 8104−8108.
(31) Hopp, T.; Zok, D.; Kleine, T.; Steinhauser, G. Non-Natural Ruthenium Isotope Ratios of the Undeclared 2017 Atmospheric Release Consistent with Civilian Nuclear Activities. *Nat. Commun.* **2020**, *11* (1), 2744.
(32) Bonamici, C. E.; Hervig, R. L.; Kinman, W. S. Tracking Radionuclide Fractionation in the First Atomic Explosion Using Stable Elements. *Anal. Chem.* **2017**, *89* (18), 9877−9883.
(33) Snyder, D. C.; Delmore, J. E.; Tranter, T.; Mann, N. R.; Abbott, M. L.; Olson, J. E. Radioactive Cesium Isotope Ratios as a Tool for Determining Dispersal and Re-Dispersal Mechanisms Downwind from the Nevada Nuclear Security Site. *J. Environ. Radioact.* **2012**, *110*, 46−52.
(34) Nucleonica. Fission Yields++. https://nucleonica.com/Application/YieldsPlus.aspx (accessed Nov 18, 2020).

https://dx.doi.org/10.1021/acs.est.1c00180
Environ. Sci. Technol. 2021, 55, 4984−4991